ACCELERATED TESTING OF METAL FOIL TAPE JOINTS AND THEIR EFFECT ON PHOTOVOLTAIC MODULE RELIABILITY

N. Robert Sorensen, Michael A. Quintana, Michael J. Mundt, Edward V. Thomas,
Steven P. Miller, and Samuel J. Lucero
Sandia National Laboratories*
P.O. Box 5800, Albuquerque, New Mexico 87185

ABSTRACT: A program is underway at Sandia National Laboratories to predict long-term reliability of photovoltaic (PV) systems. The vehicle for the reliability predictions is a system performance model, currently being run under a simulation software called GoldSim™. The model includes inputs for module performance, irradiance, and degradation. In order to be truly predictive, physics-informed degradation processes and failure mechanisms need to be included in the model. This paper describes accelerated life testing of metal foil tapes used in thin-film PV modules, and how tape joint degradation, a possible failure mode, can be incorporated into the model.

Keywords: Photovoltaic reliability, metal foil tape, accelerated testing.

1 BACKGROUND

A vibrant photovoltaic industry has emerged in recent years primarily as a result of exponential market growth, dynamic changes in technologies, and innovative approaches to what the ideal business model(s) will be in the future. The reliability of photovoltaic systems has continued to be a dominant concern of the supply chain, from materials manufacturers to component manufacturers to system integrators, and finally the end customer. Increasingly savvy customers are asking for increasingly sophisticated and complex information as due diligence is performed prior to investing massive amounts of capital. Indeed, the photovoltaics industry is no longer a cottage industry, but as maturation occurs so do growth pains and challenges.

One such challenge is to develop predictive capabilities to evaluate potential failure modes and the probability of failures in photovoltaics and apply this knowledge to predict service life. One set of tools that assists in answering the challenge are accelerated life tests (ALTs). Comprehensive ALTs provide predictive information as well as the ability to translate the information into materials specification and cost effective designs of components and systems. Finally, carefully developed ALTs assist in the development of improved product integrity and shorter time-to-market development cycles.

ALTs are not yet standardized in the photovoltaics arena. It is important to remember that qualification tests, the most common type of accelerated tests recognized, do not provide a probability of failure; ideally the qualification test is meant to be passed. ALTs are destructive tests meant to uncover expected failures and provide an understanding of the physics of failure; and furthermore to develop a statistical base from which to make predictions. The study described in this paper is an initial application of accelerated life testing to a single packaging element used in some thin-film photovoltaic designs with an expectation of a much more rigorous application of ALTs in the future. [1]

Packaging of a thin film PV technology was selected to demonstrate how materials degradation phenomena can be included in the system performance model. One high likelihood failure process identified through a Failure Modes and Effects Analysis (FMEA) of the thin-film technology was degradation of the metal foil tape joints. The joints, created as a method of taking current of a thin-film device, are made by applying a metal foil tape with a pressure sensitive adhesive to the device. To generate degradation data, accelerated tests were run on samples with overlapping tape joints. Models relating the increase of resistance across the tape joints to exposure time were derived from the experimental data. These models are being incorporated in the overall system model.

2 TAPE ANALYSIS

Three tapes (designated A, B, and C) were selected for this study. They consist of one embossed and two smooth metal foils tapes. In all instances, the base metal is Cu and is plated with solder. All three tapes contain conductive particles in the adhesive.

An analysis of the conducting particles was performed using an SEM with Energy Dispersive Spectroscopy (EDS) capabilities. Figure 1 shows a back-scatter image for the conductive particles in tape A and the corresponding elemental map obtained through EDS analysis. The particles are irregular in shape, and appear to be somewhat agglomerated. The particles appear to be silver-plated copper.

Figure 2 shows an SEM image for tape B and the corresponding elemental map. The agglomerated particles are on the order of 10 microns in size, and consist of Ag-plated Cu.

Figure 3 shows a particle from tape C and the corresponding elemental map. This particle is roughly the same size (5-10μm), but in this case, it appears to be a glass sphere that has been Cu/Ag plated.

*Sandia is a multiprogram laboratory operated by Sandia Corporation, a Lockheed Martin Company, for the United States Department of Energy's National Nuclear Security Administration under contract DE-AC04-94AL85000.

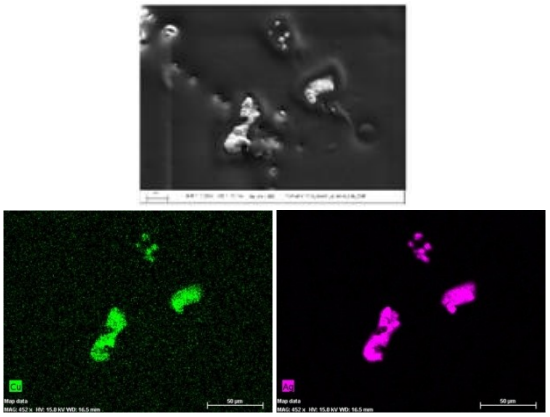

Tape A (smooth)

Figure 1. Back-scattered SEM images of the adhesive side of tapes A and B showing the conductive particles.

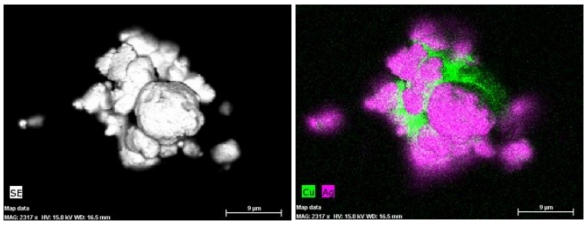

Tape B (embossed)

Figure 2. SEM image and elemental map for conductive particles in tape A.

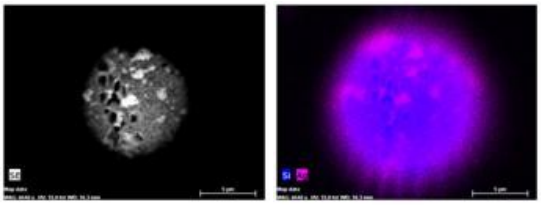

Tape C (smooth)

Figure 3, SEM and elemental map of conductive particle in tape C.

3 ACCELERATED TESTING

Test samples were designed to allow measurement of the interfacial resistance of individual tape joints. The tape was applied to a glass substrate and a second section of tape was applied over the first. Wires were soldered to the ends of the tape in order to monitor the resistance of the tape joint. A four-lead resistance system was used, eliminating the resistance of the cabling. A Keithley 100 channel scanner was used to cycle through individual tape joints, and the resistance was measured with a Keithley model 480 multi-meter. In this fashion, up to 10 identical tape joints were monitored for a given set of conditions, providing information on the uncertainty associated with the degradation process.

Samples were exposed to two types of environmental conditions - cyclic temperature (-40°C to +60°C, no humidity control) and damp heat (60°C, 70% RH). For thermal cycling, a ramp rate of approximately 7 °C/min was used, resulting in just over two cycles/hour.

3.1 Damp Heat

Samples exposed to 60°C, 70% RH exhibited fairly rapid degradation (increased electrical resistance). The results of the three tapes exposed to this environment are shown in Figure 4. Tape B (embossed) exhibited the best behavior in this environment, with almost no increase in of resistance. Tape A (smooth) exhibited substantial degradation, with resistance values above 100 ohm being observed. An intermediate response was obtained from tape C (smooth), where resistance values increased slightly, but remained below 1 ohm in value.

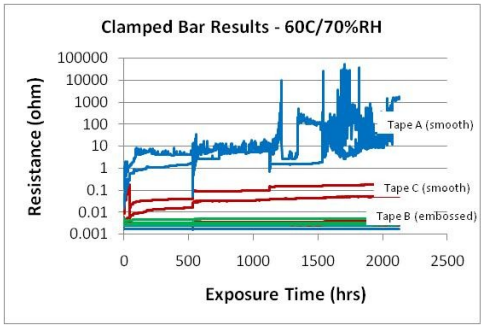

Figure 4. Resistance data for tapes exposed to damp heat (60°C, 70% RH). A bar was clamped over the tape joints to prevent total delamination (maintaining a mechanical connection).

Figure 5 shows the results of the same test when no pressure is applied to the tape joint. In this case, all three tapes exhibited unsatisfactory behavior, with resistance values above 100 ohms common.

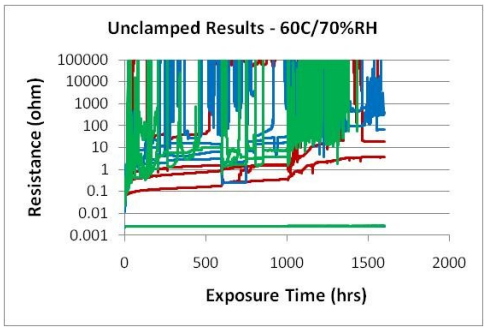

Figure 5. Resistance data for tapes exposed to damp heat (60°C, 70% RH). No clamping pressure was applied to the tape joint.

3.2 Thermal Cycling

Thermal cycling tests were performed to simulate the effect of cyclic temperature on the tape joints. The primary effect is believed to be due to differences in thermal expansion coefficient between the tape and the substrate. Two effects were observed. First, the resistance changed with temperature, with the higher resistance being observed at elevated temperature. Second, an increase in the "background" resistance was observed with increasing number of thermal cycles. It is this second effect that is being incorporated into the performance model.

Figure 6 shows data for the three tapes exposed to the thermal cycling environment. A range of responses can be seen, with some of the tape joints experiencing significant increases in resistance. The figure includes data from tapes A and B. There may be a slight improvement in performance due to the embossing, but it does not appear to be substantial. Both tapes exhibited significant increases in resistance. Importantly, as indicated above, the data represent a range in responses that must be addressed when modeling performance.

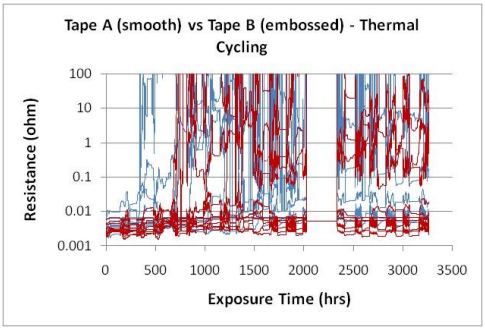

Figure 6. Comparison of tape A (smooth), shown in blue and tape B (embossed), shown in red.

Figure 7 shows the range in responses obtained from tape A during thermal cycling. These data make it clear that a "stochastic" element exists for this degradation mode, and that it must be incorporated into any degradation or performance model for the system.

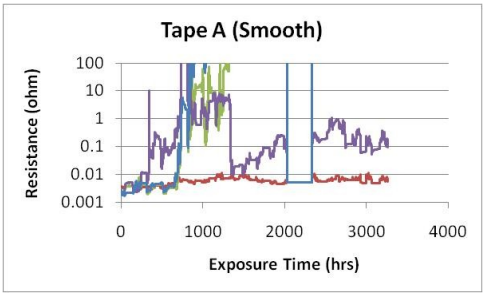

Figure 7. Selected curves from one sample (tape A-smooth) showing range of responses.

4 PERFORMANCE MODELING

System performance was modled using the commercial software tool, GoldSim™, which enables sensitivity analyses for complex definitions of reliability, as well as the modeling of environmental influences such as geographical location, seasons, and weather on the kilowatt hour output of the inverter-array over time.

The reliability modeling in GoldSim™ is configured as a parent-child hierarchy that follows the flow of kilowatt hour production through critical components in the system. The basic blocks in the model, were based on the major components of the system and the level of identification of field failures in the reporting process. All of the blocks are implemented in the GoldSim™ model using field failure and repair data to populate associated life distributions and repair distributions for each block.

There are several improvements that are implemented in the GoldSim™ model. Fidelity of both inverter and photovoltaic module modeling is improved. In GoldSim™ the scale parameters of the irradiance, failure, degradation, and inverter disturbance distributions are varied during the simulation. A sensitivity analysis supporting an improved definition of reliability is included, as well as the modeling of environmental influences such as geographical location, seasons, and weather on the cumulative kilowatt hour production of the inverter-array over time. Thus, the implementation in GoldSim™ should represent significant improvement in the fidelity of the effective availability metric, which can be directly compared to what is used by the utility operators. Effective availability is defined in terms of actual kilowatt hour production compared to what could have been produced if the inverter array was perfectly available for the weather conditions at a particular geographical location.

In order to assess the effect of tape joint degradation on system reliability, a link between performance and tape joint contact resistance must be established. In a thin film module, conductive tape can be used to collect current from the cells, and is used as an electrical connection to both the first and last cell of the module. As the tape joint degrades, it can be represented as a parasitic resistor in series with the module.[2,3] This simple circuit represents a single module. Any increase in resistance in that joint is manifest as an increase in circuit series resistance for the module. Multiple modules can be strung together in series, with the tape joints represented as two resistors between each module. This representation allows us to assess the effect of tape degradation on system performance, and is necessary in order to include this kind of degradation in the system reliability model.

A statistical model relating the increase in resistance to exposure time was developed using the experimental data that are displayed in Figure 8. This model was incorporated in the system simulation. Analysis of the data indicated that the growth in log(R) was approximately linear with $t^{0.5}$, where t is the number of cycles. For any given point in time, the distribution of log(R) across joints was modeled with a normal distribution. Thus, the overall statistical model that was developed is of the form:

$$Log(R\ (t)) \sim Normal\ (\mu(t), \sigma),$$

with mean given by $\mu_t = a + bt^{0.5}$, and standard deviation σ that is independent of t.

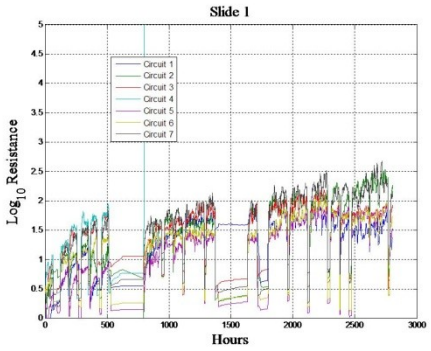

Figure 8. Tape joint response used for system simulation.

To calculate the effect of the parasitic resistance on module performance, a simple electrical system analysis was performed. In general, the electrical properties of a module can be used to calculate the effect of resistance on performance. To illustrate this, three modules were considered. First is a "standard" module with a 70 watt output, and a max power point voltage of 40V. (Two other cases are considered: a 300W, 50V module and a 73W, 33V module.) The current for the standard module, based on these values, is 1.75 A. Connected through an external load and running at peak power, the resistance of the external load (R_{load}) is 22.86 Ω (R = E/I). Parasitic resistances (R_{tape}) were then introduced into the circuit

(one for each tape joint on the module). Combining these with R_{load} provides a total resistance. Assuming that the voltage remains constant across the module, a new current can be calculated, and then used to calculate the power dissipated through the external load and through the two tape joints. The available output power then becomes that consumed by the external load. A decrease in power can be calculated as the ratio P_{load} to $P_{load\text{-}initial}$. We then fit the curve of relative power vs. resistance to obtain an analytical solution that can be programmed into the performace model (the equation used to fit this curve has no physical significance – it is merely a mathematical description of the generated data). For the "standard" module, the description is:

Relative Power= 0.1734+0.819*EXP(-R/5.11)

Using accelerated aging data generated during thermal cycling of the tape joints, a description of the resistance as a function of thermal cycles can be obtained. If we assume a diurnal cycle and no shading due to clouds, a description of resistance as a function of time is derived.

$$R(t) = 10^{(a+b\sqrt{t}+e)}$$

Where *a* is the initial resistance at t=0, *b* is the slope (in this case 0.028) obtained from the thermal cycling tests, and *e* is a "unit-specific" random normal variable with mean of zero and a standard deviation of 0.3. In this example, the initial resistance is already included in the module specifications. Thus, we set a to zero as we are interested in the resistance increases, and. For this example, the equation then becomes:

$$R(t) = 10^{(0.028\sqrt{t}+e)}$$

These calculations include the assumption of two parasitic resistors for each module (top and bottom). The tape interface on the test sample is smaller than on the module (factor of 20), so the calculations need to be corrected for area. The longer tape interface on the module can be treated as 20 parallel resistors so the actual parasitic resistance for the module is reduced by a factor of 20.

Thus, two equations are needed for the simulation. The first is the one that describes module power as a function of resistance. It is combined with the equation that gives resistance as a function of time. For the simulation, each module is assigned a specific equation for R = f(t). That is, a unique value for "e" is assigned based on the assumed normal distribution of e (zero mean and standard deviation of 0.3). That value remains constant (for that module) throughout the realization, and is used to determine the decrease in output power for the module.

In this simulation, the acceleration factor (time compression) based on one thermal cycle per day is likely unrealistic. Each thermal cycle covers the entire temperature range of -40°C to +60°C. A more realistic representation may be that 200 cycles is the equivalent of 5 years on the field. The process depicted here allows the use of either.

Figure 9 shows the effect of module design in this simulation. Note that as the wattage of the module increases, the effect of resistance becomes more pronounced.

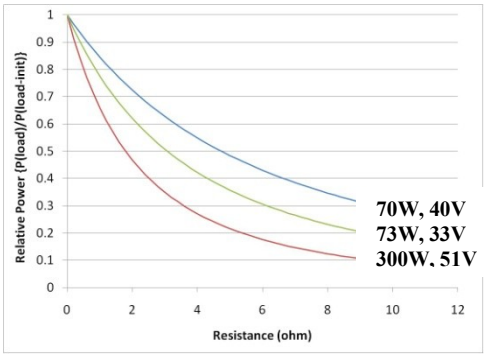

Figure 9. Calculated relative power as a function of tape resistance. Three modules are depicted.

Figure 10 shows the mean value of module degradation in this scenario. The value of "e" was set at 0, the acceleration factor used was based on 200 cycles representing 5 years, and three modules are depicted. The worst case in this situation is for the 300W module, which exhibits a degradation of approximately 20% after 25 years.

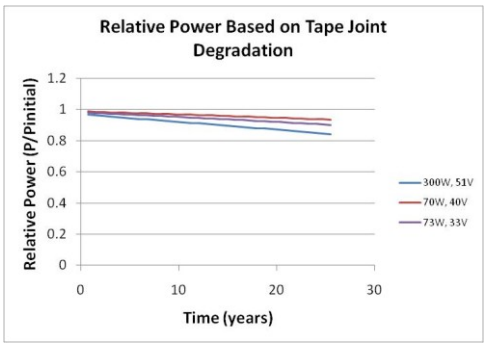

Figure 10. Calculated module degradation due to tape joint resistance. Three modules are depicted.

Figure 11 shows the degradation curves for 200 cycles/5 years, with curves for the mean (red), 1 sigma (blue), and 2 sigma (green). These curves represent the distribution that is sampled in GoldSim™ for degradation rates for each module. A smiliar set of curves are shown in Figure 12 for the case where the acceleration factor is based on 1 cycle/day. In this case, the degradation is more extensive, but the overall process and trends remain the same.

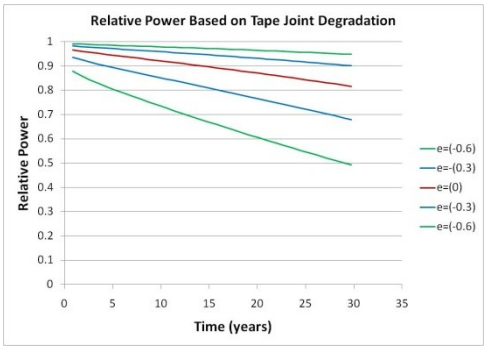

Figure 11. Distribution of responses – based on 200 cycles = 5 years

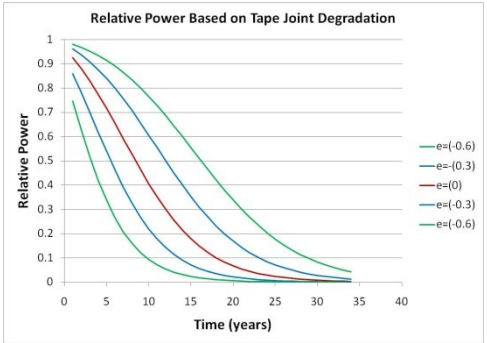

Figure 12. Distribution of responses – based on 1 cycle/day

Figure 13 is an output from the GoldSim™ simulation showing the effect of tape joint degradation on performance. The simulation was for a PV array with 450 modules and a single inverter. It includes all of the field data associated with the PV field, but it also includes specific module degradation phenomena. The plot shows the cumulative energy (kW-hr) produced as a function of time. Tape joint degradation is included as an additional "de-rating" of the module, and results in decreased output. Based on the results of the accelerated aging tests, each module is assigned a degradation rate, which is carried through the simulation. The upper curve includes a standard module degradation rate of 0.5%/year. The lower curve includes this value, as well as module degradation due to tape joint degradation. Importantly, these results are based on distributions, and represent the stochastic rather than deterministic performance.

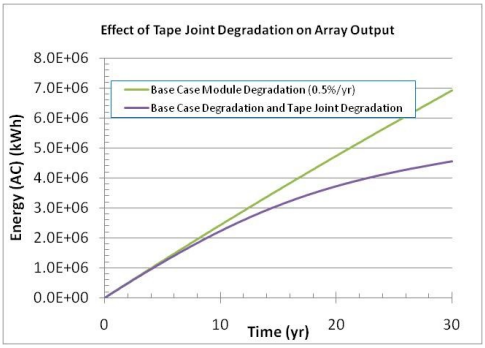

Figure 13. Simulation results from GoldSim™ performance model. The two curves represent the predicted performance with and without tape joint degradation.

5 SUMMARY

In this paper, we have shown the predicted effect of conductive foil tape degradation on module performance / reliability. The thermal cycling test represents fielded modules that undergo diurnal temperature cycling. The resulting resistance change was related to module performance through a simple electrical system model using parasitic resistors to simulate tape joint contact resistance. Through this example, we demonstrated how materials degradation data can be used in a system performance model to predict system reliability. Although this is only an initial demonstration of the process, and is therefore not complete, the utility of the technique is evident. In addition, by exercising the entire process, from accelerated aging experiments through the final system model, it becomes much easier to identify and prioritize design and processing issues. Ultimately, accelerated life tests are essential to provide long-term predictions of PV reliability, availability and performance when analyzed in conjunction with real-world operations and failure data.

6 REFERENCES

1. E. Suhir; "Accelerated Life Testing in Microelectronics and Photonics, Its Role, Attributes, Challenges, Pitfalls, and Its interaction with Qualification Tests", IEEE Polytronic 2002 Conference.
2. http://zone.ni.com/devzone/cda/tut/p/id/7230, "Photovoltaic Cell I-V Characterization Theory and LabVIEW Analysis Code".
3. D. L. King, J.K. Dudley, and W. E. Boyson, "PVSIM : A Simulation Program for Photovoltaic Cells, Modules, and Arrays", 25th PVSC; May 13-17, 1996.
4. E. Collins, M. Dvorack, J. Mahn, M. Mundt and M. Quintana, "Reliability and Availability Analysis of a Fielded Photovoltaic System," 34th IEEE PVSC Conference, June 7-12, 2009.